STEVENS INSTITUTE OF TECHNOLOGY

CASTLE POINT STATION
HOBOKEN, NEW JERSEY 07030

DEPARTMENT OF PHYSICS

UNCLASSIFIED

Proximity Effect Between Superconducting and Normal Metals

Semi-Annual Report

April, 1972

Hans Meissner

NASA Grant No. NGL 31-003-020

Office of Research Grants and Contracts

Office of Space Science and Applications

National Aeronautics and Space Administration

Washington, D. C. 20546

UNCLASSIFIED

Stevens Institute of Technology

Department of Physics

Castle Point Station

Hoboken, New Jersey 07030

Proximity Effect Between Superconducting and Normal Metals

Semi-Annual Report

April, 1972

Hans Meissner

NASA Grant No. NGL 31-003-020

Office of Research Grants and Contracts

Office of Space Science and Applications

National Aeronautics and Space Administration

Washington, D. C. 20546

Abstract

The SNS junctions studied during this period were limited to having gold (N) layers of less than 3000 Å in order to avoid that the tin (S) films become normal under the influence of the signal current, I_2, in the gold. The gold (N) layer has been alloyed with 10 wt% copper to shorten its electronic mean free path which increases the tin layer critical current while decreasing the Josephson critical current. It has also been found that a previously-reported anomalous voltage shift in the presence of I_2 is caused by the tin being driven normal. After deposition, the samples are now transferred to a conventional cryostat to provide better thermal contact to the films. This reduction of heating in the films produced more linear I-V characteristics and a change in the constant-voltage current gain, α_o. While, previously, α_o showed a linear dependence on I_2, it is now, at least for I_2 not too small, more independent of I_2.

In order to achieve power gain the SNS device must (a) be operated at lower temperatures where the effects of fluctuations are less, and (b) be constructed such that the input resistance is much reduced and the dynamic output resistance increased. A much improved geometry is proposed for immediate trial using a more sophisticated evaporator.

Introduction

A Josephson junction is a device wherein two superconductors are separated by either an insulating or normal metal barrier. Henceforth the junction with the insulator will be termed SIS and the one with the normal metal barrier SNS. The barrier thickness is critical to the operation of the device (e.g. the normal metal barrier may be as thick as 10,000 Å, whereas the insulating barrier is restricted to thickness less than 50 Å). The effect of the barrier is to provide a weak coupling between the phase of the Cooper pairs in one superconductor with respect to that in the other superconductor.

The present geometry consists of a sandwich of films, with tin forming the outer two superconducting layers and gold the normal metal barrier. It is in the form of two crossed "legs" of tin with a gold film between them. (See Fig. 1, page 3.)

Previously, the films were deposited in a dual evaporator/cryostat (see NASA report SIT-P243 (10/69) for a complete description), originally onto a helium-cooled substrate, later onto a 273K substrate which was immediately cooled to liquid helium temperatures, and their electrical characteristics measured in situ without breaking the vacuum. The present procedure is far less restricted in its capabilities.

The "superconducting transistor" is a three-terminal device wherein the Josephson current is modulated by the introduction of a signal current directly into the normal metal barrier and returned through one of the tin legs. The realization of gain from the device is presently limited by the resistance levels heretofore encountered with the existing geometry.

A. Thin Films

During the last report period 10 experimental runs were effected with the tunneling barrier thickness, t_n, ranging from 600 Å to 3000 Å. These SNS films were vapor-deposited onto a single-crystal sapphire substrate at 273 K. Previously, the films were cooled to helium temperatures immediately after deposition and their I-V characteristics measured in situ. This method of cooling the sample to cryogenic temperatures was limited in that the SNS films were making thermal contact to a liquid helium reservoir through the single-crystal sapphire substrate, the copper substrate holder, some indium washers, and the copper bottom of the helium vessel. In spite of the high thermal conductivity and large contact-areas, there still existed too large a temperature gradient from the thin films to the helium reservoir when Joule heating occurs in the junction.

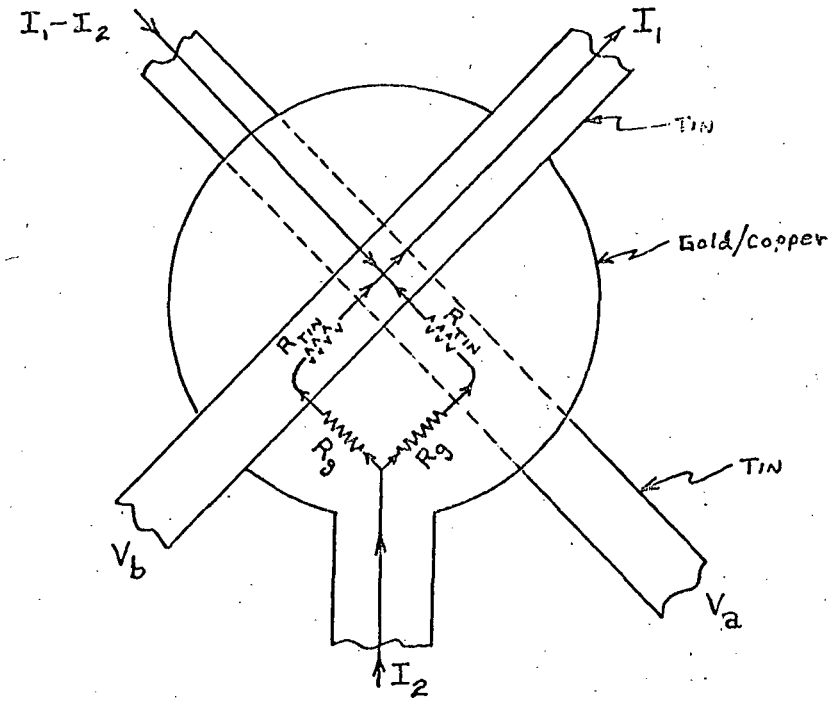

Fig. 1. Present geometry of SNS films illustrating current paths as well as gold path resistance, R_g, and normal state tin leg resistance, R_{tin}.

This procedure has been changed to: (a) vapor-depositing the SNS films in the evaporator/cryostat and then (b) transferring the sample to a conventional cryostat for complete immersion in liquid helium. It was found that this method removed some of the rounding of the I-V curves and decreased the variation of α_o with signal current (see section E) resulting in a more linear device. The present system requires the films to be at 300 K no more than 30 minutes before cooling to liquid nitrogen temperatures.

For reasons explained in section D, it became desirous to decrease the gold layer electronic mean free path, ℓ_n, and hence the Cooper pair coherence length in the gold, ξ_n, which is given for the "dirty" metal case ($\ell_n \ll \xi_n$) by[1] $\xi_n = (\hbar v_n \ell_n / 6\pi kT)^{\frac{1}{2}}$, where v_n is the Fermi velocity of the electrons in the normal metal, and T is the absolute temperature. The values of ξ_n and ℓ_n were decreased by alloying the heretofore 99.99% gold with 10 wt.% of copper.

Typical values for the gold film parameters with and without the copper impurity are shown in table I. The films of tin were left unchanged and were typically 9000-10,000 Å thick with electronic mean free paths of $\ell_{sn} \sim 4000$ Å.

Table I

	pure gold	gold/copper alloy	
sample no.	26	29	27
thickness	1100 Å	600 Å	1700 Å
ℓ_n	500 Å	120 Å	160 Å
theoretical ξ_n(3 K)	1000 Å	470 Å	550 Å
resistivity	4.4×10^{-6} Ω cm	11.5×10^{-6} Ω cm	9×10^{-6} Ω cm

1. G. Deutscher, P. G. deGennes, Superconductivity (Marcel Dekker, Inc., N.Y.) 1969, edited by R. D. Parks, pg. 1006.

B. Current Voltage Characteristics

The I-V characteristics for various values of the barrier current, I_2, are shown in Fig. 2. The I-V characteristic for the junction not immersed in liquid helium shows more rounding of the curves as current is increased and a suppressed increase of I_1 due to I_2. (The negative slope at the

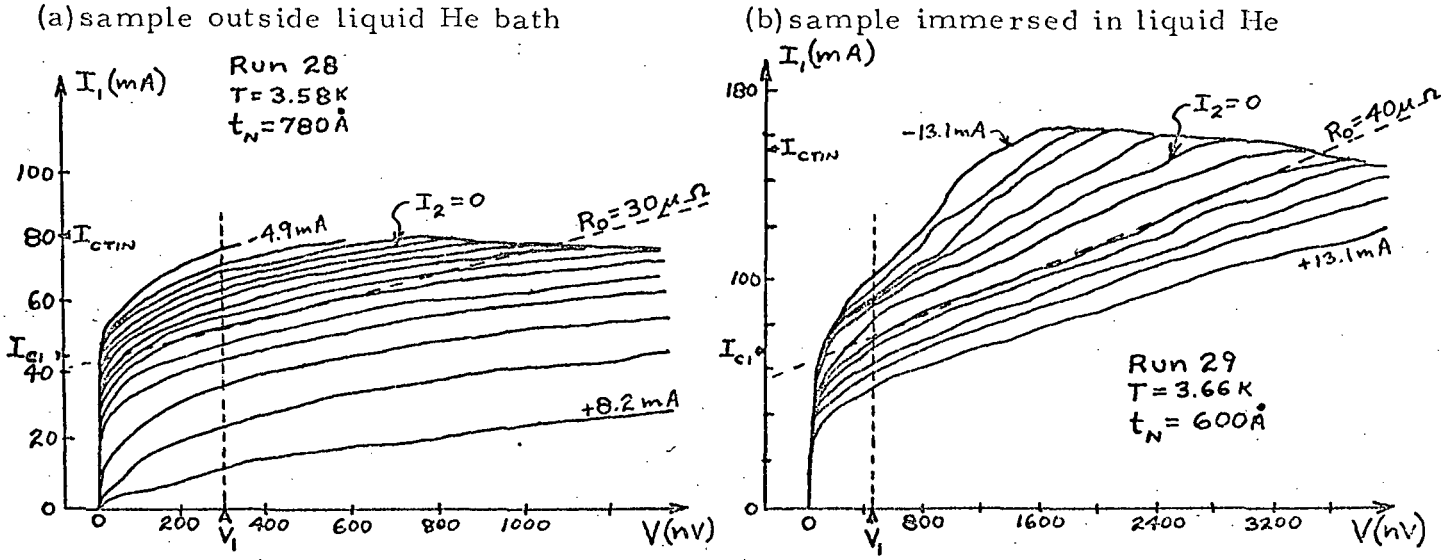

I_2 values (mA) for curves from top to bottom; $I_2 > 0$ for I_2 parallel to I_1:

(a)				(b)		
-4.9	0.0	3.3	6.5	-13.1	0.0	9.8
-3.9	0.8	4.1	7.4	-9.8	3.3	11.5
-2.3	1.6	4.9	8.2	-8.2	6.5	13.1
-1.1	2.5	5.7		-3.3	8.2	

Fig. 2. I-V characteristics of SNS junction illustrating heating effect and tin critical current.

top of the I-V curves is due to the tin leg going normal and adding its resistance to the load of the current supply causing the current to drop somewhat.)

Two important parameters of the device found in Fig. 2 are (1) R_o, the small-signal, low-frequency dynamic output impedance of the device found as the inverse slope of the I-V characteristic and (2) the constant-voltage,

small-signal, low-frequency current gain $\alpha_o \equiv (\Delta I_1/\Delta I_2)_{V_1=\text{const.}}$ which is calculated for a given V_1 on the I-V graph.

In a previous report it was mentioned that voltage shifts of an unknown origin were occasionally observed in the presence of I_2. It is now believed that

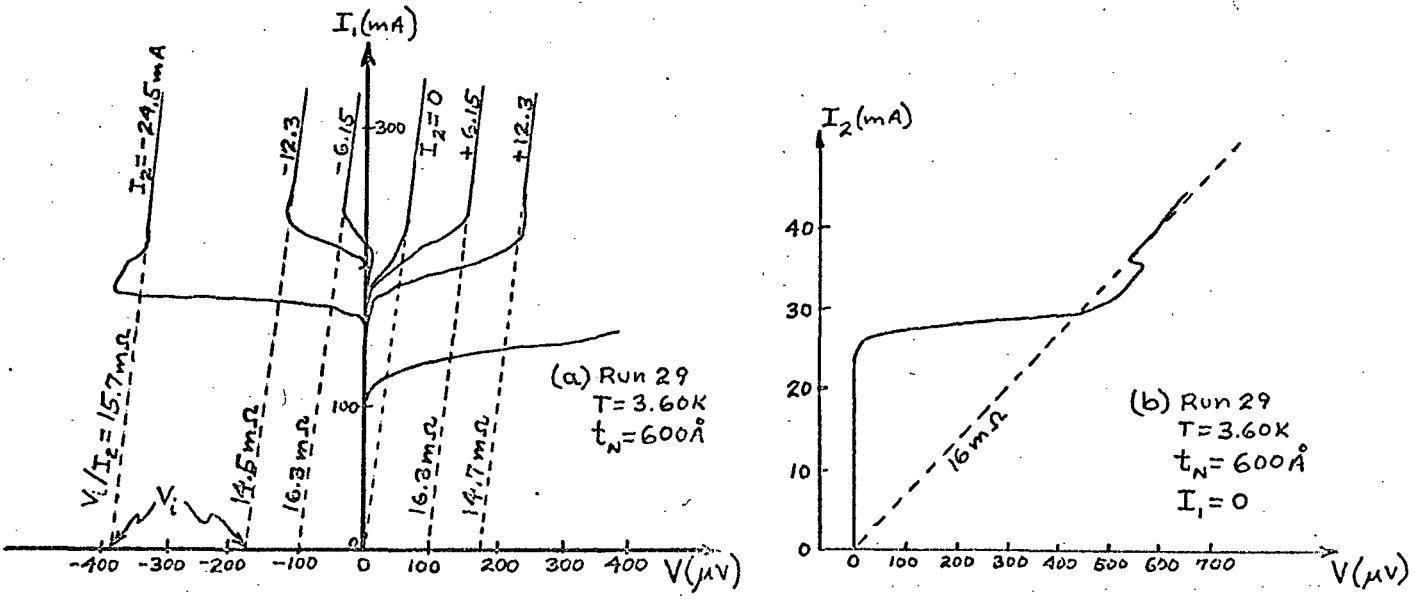

Fig. 3. (a) I-V curves at large currents showing the voltage shifts proportional to I_2. (b) I_2 versus V for $I_1 = 0$.

this excess voltage (shown as V_i in Fig. 3a) is due to the $I_2 R_{tin}$ potential drop across that portion of the tin voltage leg in proximity to the gold which carries I_2 (see Fig. 1 for R_{tin}). The calculated resistance of that portion of the tin voltage leg in proximity to the gold agrees well with both the observed voltage shift (Fig. 3a) divided by I_2 and also with the normal resistance of the I_2 versus V curve with $I_1 = 0$ (Fig. 3b).

C. Effect of External Magnetic Field

The effect of a magnetic field, H_e, on the supercurrent density, j, in a Josephson junction without self-field limiting is given by[2]

$$j = j_c \sin [2\pi H_e \, d\chi/\Phi_o + f(v)], \qquad (1)$$

where j_c is the critical suppercurrent density, $d = 2\lambda_L + t_n$, λ_L is the London penetration depth in the tin, χ is the distance along the junction perpendicular to H_e, w is the junction width, Φ_o is one quantum of magnetic flux, and f(v) denotes the dependence of the Josephson current on voltage.

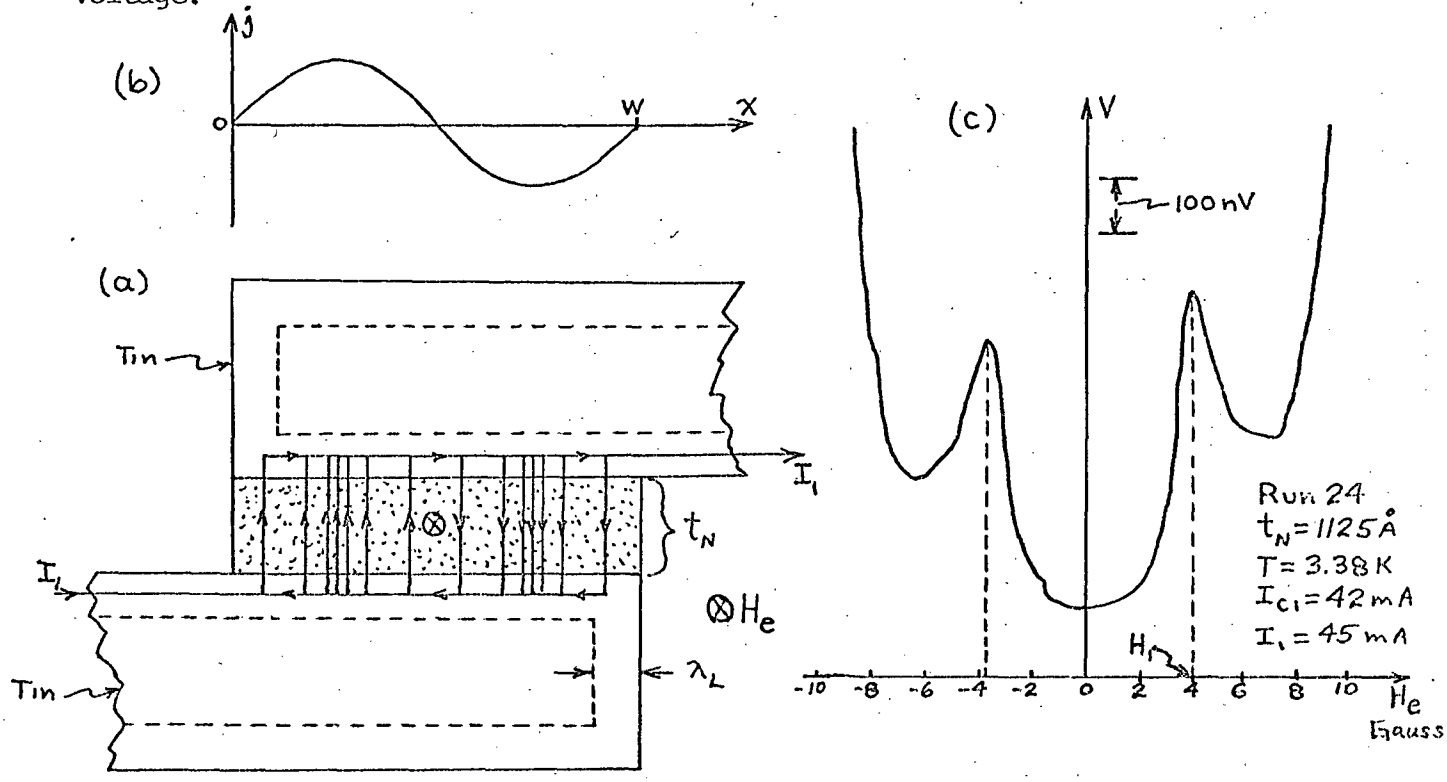

Fig. 4. (a) SNS junction with one quantum of flux inside, (b) the current density across the junction, (c) V versus H_e for $I_{c_1} \lesssim I_1$.

2. B. D. Josephson, Adv. Phys. 14, 419 (1965).

Fig. 4a shows a junction when $H_e = H_1 = \Phi_o/d$. Equation (1) then gives the sinusoidal variation of current density with χ as shown in Fig. 4a and b. The net current for this case is zero, but there exists a non-zero circulating current in the junction as seen in Fig. 4a. The flux enclosed within this circulating current is one quantum, Φ_o. Whenever the flux in the junction area is an integer multiple of Φ_o the total current in the ideal 2-dimensional case will be zero.

Fig. 4c is an experimental graph of junction voltage versus external magnetic field H_e with $I_{c1} \lesssim I_1 < I_{ctin}$, where I_{c1} and I_{ctin} are the Josephson and tin critical currents respectively. Although the nodes are somewhat "washed out" by the addition of quasiparticle current (excited single electron and hole current) to the supercurrent, they still represent the minima in total supercurrent as reflected by Eq. (1). If this curve were repeated for $I_1 > I_{ctin}$, the nodes would be lost, because essentially all of the current is quasiparticle current by then, and the quantum mechanical effects of the junction are seen only in the supercurrent tunneling state.

D. Josephson Critical Current and Tin Critical Current

The Josephson critical current has been found to vary with temperature as $I_{c1} \propto (1-t)$ for $t = T/T_{cSNS}$ not close to one, where T_{cSNS} is the zero-current transition temperature of the SNS junction. In addition to the Josephson critical current there exists another critical current as seen in the I-V traces of Fig. 2. This second critical current is a manisfestation of one of the tin "legs" in proximity to the gold becoming normal conducting. The temperature dependences of both the tin critical current, $I_{ctin} \propto (1-t)^{\frac{1}{2}}$,

as well as the Josephson critical current are qualitatively but not quantitatively the same for the new short mean-free-path samples immersed in liquid helium as for those in previous reports. See NASA report SIT-P263 (10/71) for a detailed description. In the past, many difficulties arose because the two critical currents were almost of equal magnitude. In the following we will discuss the measures which have been taken to decrease the Josephson critical current while increasing the tin critical current.

Although Rockefeller[3] and others[4] have observed Josephson currents with barrier thicknesses greater than 7000 Å, we had been restricted to gold films less than 2000 Å because for thicker gold films, with large mean free paths, the tin critical current became less than the Josephson critical current and, hence, destroyed the operation of the SNS device.

For a "dirty" system ($\ell_n << \xi_n$) near its transition temperature, the critical current of a SNS junction is given by[4]

$$I_{c_1} \alpha \xi_n \exp(-t_n/\xi_n), \qquad (2)$$

where t_n is the normal metal barrier thickness and the other terms have been defined in section A. Equation (2) clearly shows that it is not the gold thickness alone which determines the Josephson critical current but the ratio t_n/ξ_n. Unfortunately, the tin critical current also decreases with the gold thickness. However, the tin is "affected" by the gold only up to a gold thickness of about ξ_n but not beyond. Thus, if we shorten ξ_n considerably, we may increase t_n beyond a few ξ_n without the tin critical current being affected further while the Josephson critical current, which

3. R. Rockefeller, NASA Report SIT-P251 (6/70)

4. J. Clarke, Proc. Roy. Soc., A308, 447 (1969)

depends upon t_n/ξ_n, is reduced much below I_{ctin}. Here, we have taken advantage of the effects of shortening ξ_n so that we might separate the two critical currents for lower temperatures where they previously had intersected on a temperature graph. The utility of lower temperatures will be explained later.

As a consequence of their large Josephson critical currents, I_{c1}, (as expected for the heretofore small t_n/ξ_n) the junctions have experienced a self-field limiting or "crowding"of the supercurrent in the junction. The parameter of this crowding effect is the Josephson penetration depth, λ_J. λ_J may be computed from either the critical current density or H_1 in Fig. 4c. These two methods of calculating λ_J provide a self-consistency check of the result. For T = 3.44 K, I_{c1} = 9mA, H_1 = 2.4 G, $\lambda_L(0)$ = 500 Å, t_n = 1125 Å we get[5] $\lambda_J = 1.2 \times 10^{-3}$cm. The width of the junction, W, is 2×10^{-2} cm; so the supercurrent is being crowded in this case. This crowding can be varied by changing barrier thickness and operating temperature. The effect of λ_J in the finite voltage region, where the superconducting transistor is to be operated, is not well defined, for here Eq. (3) must be solved analytically to determine the d.c. characteristics of the junction.

$$\lambda_J^2 \frac{\partial^2 \phi}{\partial \chi^2} = \sin \phi + \frac{\hbar}{2eRI_c} \frac{\partial \phi}{\partial t} \qquad (3)$$

ϕ is the Cooper pair wave function phase difference across the junction and χ is the distance along the width of the junction. The variation of the IV characteristic, and hence R_o, with λ_J is yet to be analyzed.

5. See NASA report SIT-P270 (5/71 for λ_J description.

E. Dependence of the Josephson critical current on I_2.

The d.c., small-signal, constant-voltage current gain of superconducting transistor, α_o, is defined by $\alpha_o \equiv (\Delta I_1/\Delta I_2)_{V_1 = \text{const.}}$ Figures 5 illustrate the variation of α_o with signal current I_2. Figure 5a shows an essentially linear increase of α_o with one direction of I_2. This effect can be explained by assuming heating in the gold barrier due to I_2 and requiring that the heat flows by conduction to the helium bath. Figure 5b shows α_o is essentially constant with I_2 in the case of immersion in liquid helium where heating effects should be much less. Figures 5 also exhibit a slight periodic variation of α_o with I_2, with period $\sim$ 5mA. This modulation can be predicted from I_2's self field effect.

(b) sample immersed in liquid He

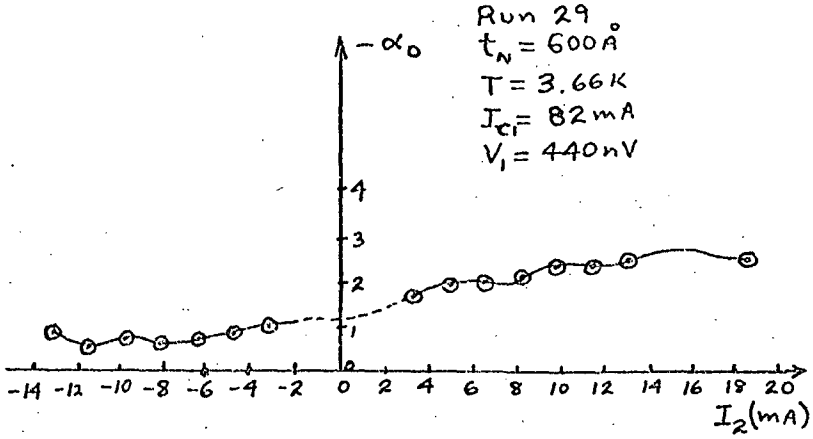

(a) sample not immersed in liquid He

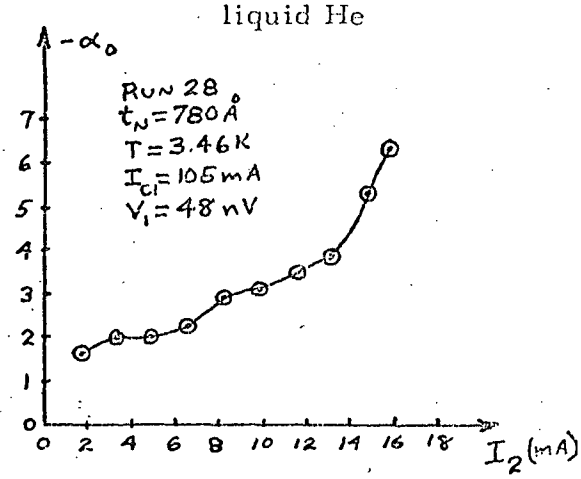

Figure 5. α_o versus I_2 for films (a) not immersed in liquid helium (b) immersed in liquid helium.

If the values of α_o obtained for different voltages, V_1, and I_2 not too small, are plotted versus V_1, we get Figure 6. Here we see that as $V_1 \to 0$, α_o approaches -0.5 for I_2 antiparallel to I_1 and $\alpha_o \sim -2$ for I_2 parallel to I_1. The variation of α_o with V_1 is due to the spreading of the I-V curves with V and is probably due to resistive dissipation in the junction area (i.e. more and more quasiparticles entering the tin and having resistive collisions before condensing into Cooper pairs). Note the larger values of $-\alpha_o$ in Fig. 5a.

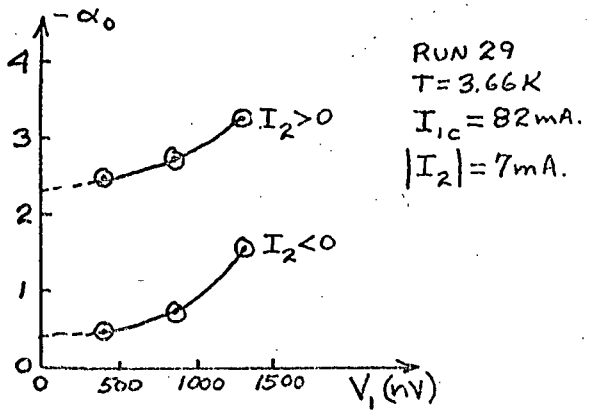

Figure 6. α_o versus V_1.

A simple argument leads one to expect $\alpha_o = \frac{1}{2}$. For the present geometry (Fig. 1) the current I_2 in the gold disc splits almost equally into the two tin legs, because the potential difference between the two

tin legs ($\sim$ 10μV) is small compared to the potential differences occurring in the gold disc (2mV). Because I_2 splits almost equally, only one half of I_2 tunnels through the entire junction while the other half of I_2 affects I_1 only by its magnetic field. This factor of 1/2 would explain the $\alpha_o = -\frac{1}{2}$ in Fig. 6 for I_2 anti-parallel to I_1. For the parallel case α_o would be expected to be somewhat larger, because the self fields should always be contributing to decreasing I_1; but the value of $\alpha_o = -2$ has yet to be satisfactorily explained.

F. Requirements for Gain

The simplest representation[6] of the SNS junction as a small-signal, low-frequency linear device yields a power gain of

$$G_p = \frac{\alpha_o^2 R_o^2}{(R_o + R_L)^2} \frac{R_L}{R_i} , \qquad (4)$$

where R_o and R_L are the output and load resistances respectively. R_i is the input resistance and is measured from a superconducting tin leg to the gold lead to the center barrier. As expected, the magnitude of α_o has been on the order of one. Thus, to obtain power gain we need to maximize the ratio R_o/R_i.

The differential resistance, R_o, of the IV slopes (see Fig. 2) in the region between the Josephson critical current and that of the tin has been of the order of 50×10^{-6} Ω. The input resistance, R_i, has been of the order of a few ohms. It can be reduced by at least two orders of magnitude through improvement of the barrier gold layer geometry (see section G). The increase of R_o requires lower temperatures where the rounding disappears.

---

6. See NASA report SIT-P270 (5/71) for the model.

Here we see the advantage of decreasing the Josephson critical current and increasing the tin critical current so that the junctions might be observed at lower temperatures. Temperatures below $T_{cSNS}/2$ will eliminate an additional series resistance[7] in the tin layers near the gold-copper alloy while also reducing fluctuations which tend to "round" the critical current knee.

The exact calculation for R_o can be done by numerically solving Eq. (5)[8,9] for dV/dI with $V \neq 0$.

$$I = \frac{G\hbar}{2e}\frac{d\phi}{dt} + \frac{C\hbar}{2e}\frac{d^2\phi}{dt^2} + I_c \sin\phi \qquad (5)$$

where $G = R_n^{-1}$ and ϕ is the difference in the phase of the superconducting wave function across the junction and is related to the total voltage across the junction by $d\phi/dt = (2e/\hbar)\ V$.

G. Planned Geometry

In principle, the input resistance of the device, R_i, which is measured across a superconducting tin leg and the gold lead to the barrier, can be reduced by a few orders of magnitude by using superconducting tin leads to the gold layer in the junction proper. Figure 7 illustrates such a proposed geometry.

---

7. J. Clarke, Phys. Rev. B4, 2963 (1971).

8. W. C. Stewart, Appl. Phys. Lett 12, 277 (1968).

9. D. E. McCumber, Jour. Appl. Phys. 39, 3113 (1968).

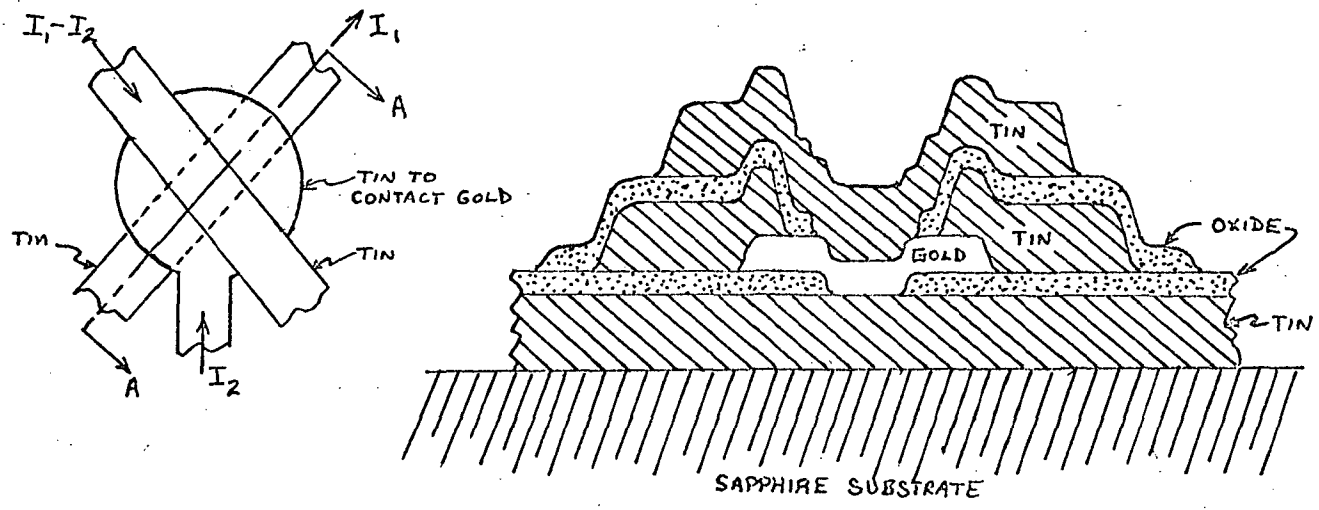

section A-A with exaggerated scales for clarity

Fig. 7. Proposed SNS junction thin film geometry showing cutaway view.

After a "leg" of tin has been deposited onto a sapphire substrate an insulating layer (e.g. SiO) is laid over the tin with the exception of a small circle which will be the tunneling area. A disc of gold-copper alloy, just slightly larger than the circle in the insulator, is then deposited. Following the barrier metal is a tin lead which will carry I_2 to the barrier with no resistance. The tin lead will have a circular "hole" somewhat larger than the size of the hole in the oxide layer, and hence will make electrical contact to the gold-copper alloy disc peripherally. Another insulating layer with a hole large enough to expose only the gold-copper alloy to the ensuing layer is deposited. A final tin leg is deposited to complete the SNS junction. The oxide layers are chosen thick enough so as to prohibit the formation of SIS tunnel junctions between the tin layers. These Sn/SiO/Sn layers do act as a capacitor, though, and if the two outer tin "legs" were made into discs the capacitance of the SNS

junction, C, could be greatly increased as is desired for increased $\beta_c = 2e\, I_{cl}\, C\, R_n^2 / \hbar$.

Instead of using the dual evaporator/cryostat described in NASA report SIT-P243 (10/69) for deposition, future films will be deposited in a Veeco Model VE400 vacuum system which has 9 positions for 9 different masks to produce the required geometry. The measurements on the samples will be performed in a conventional cryostat. This method not only allows greater flexibility but also comes close to the situation encountered in the practical use of the device.